Chemistry–A European Journal
Research Article
doi.org/10.1002/chem.202302585
Chemistry Europe
European Chemical Societies Publishing
www.chemeurj.org

A Living Topochemical Ring-Opening Polymerization of Achiral Amino Acid N-Carboxy-Anhydrides in Single Crystals

Matthias Rohmer,[a] Stefan G. Ebbinghaus,[b] Karsten Busse,[c] Julian Radicke,[c] Jörg Kressler,[c] and Wolfgang H. Binder*[a]

A living topochemical ring-opening polymerization (ROP) of achiral amino-acid N-carboxyanhydrides (NCAs) is reported. Single crystals of the NCAs of α-aminoisobutyric acid (Aib) and 1-aminocyclohexanecarboxylic acid (ACHC) were grown, allowing a ring-opening polymerization macroscopically induced by amines. The single crystals could be polymerized at temperatures from 25–50 °C after physically contacting the amine-based initiator with the crystals. Topochemical polymerization of the crystals was proven by MALDI-ToF MS and XRD, generating polymers with chain lengths of up to 40 units and a complete affixation of the initiating amine at the polymer's head. Due to the proper alignment of the reacting groups in the crystal, longer polymer chains with improved purities can be reached, as chain-transfer is reduced as compared to solution polymerization. Simple purification of the polymers can be achieved by separation of the unreacted NCA via dispersion in acetonitrile. Overall, this method enables the preparation of polymers with higher chain length and purities at mild conditions, finally demonstrating a crystal-based ring opening polymerization.

Introduction

Topochemical polymerizations are attractive and promising methods to generate materials with a high degree of ordering, programmed by the starting arrangement of monomeric units in the crystal's 2D/3D-space. Nearly exclusively these reactions are based on addition chemistries, such as [2+2] and [4+4] cycloadditions,[1] azide-alkene/alkyne reactions,[2] Dies-Alder reactions[1a,3] or the polyaddition-chemistries of dienes or diynes.[4] Typical triggers for such reactions are light,[5] temperature[4b] or pressure,[3,6] potentially allowing the preparation of polymer single crystals, which cannot be generated by other methods.[7] By introducing supramolecular interactions (e.g. hydrogen bonds[8] or π-systems[9]) the crystal lattice can be organized favorably to promote topochemical polymerization by preorganization of the involved functional groups.[10] This demonstrates the importance of interplay between crystal engineering[11] and polymer science, as the spatial arrangement of the involved reactive centers in the crystal lattice and their distances then define the reactivity of such topochemical reactions. Thus, besides a suitable distance of about 3–5 Å between the reactive moieties, a favorable topological arrangement of functional groups in the resulting final material must fit. The preorganization of two monomers in the same crystal lattice[12] can result in easily obtainable alternating copolymers, which is another unique feature of topochemical polymerizations.[13] Chemistries besides addition reactions are rare in topochemical polymerizations, especially when considering chain growth-polymerizations such as the ring-opening polymerization (ROP) of N-carboxyanhydrides (NCAs). ROP of NCAs is enabling the preparation of a vast variety of poly(amino acids) but is usually conducted in solution.[14] Early reports of the ROP in single crystal NCAs are featuring L-leucine-NCAs, displaying a distance of 4.407 to 6.760 Å between the amine group and the carbonyl group next to the α-carbon atom of the NCAs, which are acting as reactive centers, leading to oligomerization and proving that a suitable topochemical arrangement for the polymerization in the crystal is required.[15] The poor reactivity of other NCAs like e.g. glycine-NCA single crystals, displaying an even lower distance of 3.907 Å,[16] emphasizes the importance of topochemical effects such as spatial arrangements of the reacting amino and carbonyl group. Thus, dimerization via hydrogen bonds hinders the movements of the glycine-NCAs, whereas in L-leucine-NCA the layered structure favors polymerization.[17] It was observed that racemic phenyl-N-carboxyanhydride[13a] lead to only minor chiral inductions upon crystal-based polymerizations, obtaining oligomers of less than

[a] M. Rohmer, Prof. Dr. W. H. Binder
Macromolecular Chemistry, Institute of Chemistry
Martin-Luther University Halle-Wittenberg
Von-Danckelmann-Platz 4, 06120 Halle (Germany)
E-mail: wolfgang.binder@chemie.uni-halle.de
[b] Prof. Dr. S. G. Ebbinghaus
Inorganic Chemistry, Institute of Chemistry
Martin-Luther University Halle-Wittenberg
Kurt-Mothes-Straße 2, 06120 Halle (Germany)
[c] Dr. K. Busse, J. Radicke, Prof. Dr. J. Kressler
Physical Chemistry of Polymers, Institute of Chemistry
Martin-Luther University Halle-Wittenberg
Von-Danckelmann-Platz 4, 06120 Halle (Saale) (Germany)

Supporting information for this article is available on the WWW under https://doi.org/10.1002/chem.202302585

10 units, as demonstrated by MALDI-ToF MS.[18] This chemistry can also be applied to oligomerize two-dimensional NCA crystals at a water-air interface.[19] Initiation by an amine at the surface of the crystal and the disturbances in the crystal lattice controlled chain growth make this polymerization a special kind of topochemical polymerization, which deviates from the previously reported topochemistry in some points.[17,20] Several L-/D-amino acid-NCAs with a layered crystal structure have been successfully polymerized using this special topochemical ROP. The use of other, e.g., smaller nonchiral amino-acid NCAs has not been reported yet.

In this article we report on the topochemical ring-opening polymerization (ROP) of N-carboxyanhydrides (NCAs) of the nonchiral amino acids α-aminoisobutyric acid (Aib) and 1-aminocyclohexanecarboxylic acid (ACHC), leading to helical polymers with a preferred screw-sense by use of chiral initiators. Using single-crystals of Aib-NCA and ACHC-NCA, we are able to conduct the ROP with minuscule amounts of neat-initiators, finally generating either left- or right-handed helices as proven by CD. We also report on the suppression of side reactions, such as chain transfer- and termination chemistries, of this living topochemical ROP, displaying enhanced chain lengths and reduced impurities as conventionally observed in solution polymerization.[21] Finally, we demonstrate the high potential of this topochemical polymerization to induce chirality by use of chiral initiators, leading to controlled either left- or right-handed helices.

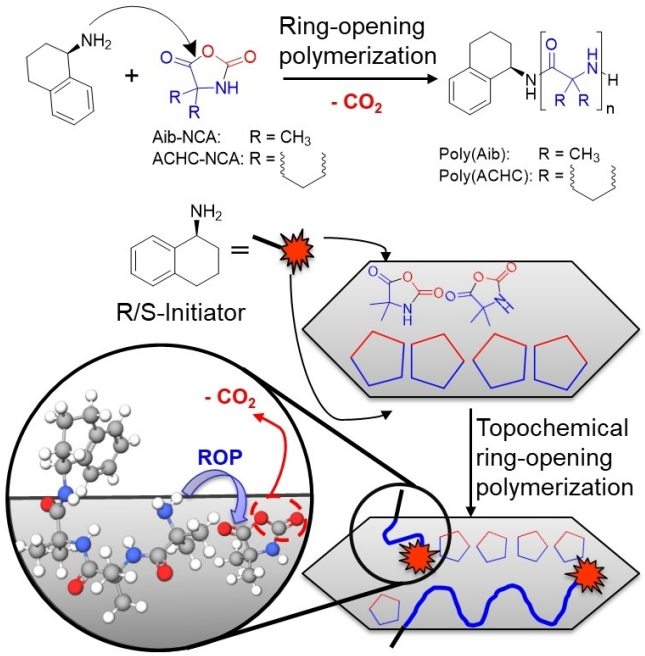

Scheme 1. Schematic overview of a topochemical ring-opening polymerization (ROP) via surface-attack initiation of an NCA single crystal, leading to chain growth through the crystal by a constant attack of the forming primary amine at the growing chain end onto the carbonyl group of the next NCA ring in the crystal lattice. ROP, initiated by 1,2,3,4-tetrahydro-1-naphthylamine in a normal amine mechanism by nucleophilic attack at the carbonyl group next to the α-carbon atom of the NCA.

Results and Discussion

To prove the polymerizability of achiral amino acid NCAs by a topochemical ROP, highly pure and ordered crystals of the respective NCAs have to be grown. Our concept relies on the initiation of polymerization at the face of the crystal, proceeding from the surface through the crystal (see Scheme 1). During polymerization CO_2 will evolve, thermodynamically driving chain growth, similar to solution ROP of NCAs. We projected that we could easily reach higher chain length and simultaneously suppress side reactions by the activated monomer mechanism and chain transfer reactions, as the polymerization is not conducted in solution, where chain length normally is limited by the poor solubility of the polymers. The pure polymer should then be easily isolated by a simple purification step after the polymerization to remove unreacted monomer and remaining initiator.

Single crystals of Aib- and ACHC-NCAs

We started our investigation with the preparation of single crystals of the two NCAs by crystallizing from a hot saturated solution. Two different approaches were probed leading to crystals of different sizes: (*Method a*) the NCA was dispersed in a small amount of ethyl acetate and heated under boiling conditions of the solvent, whereafter a small amount of ethyl acetate was added until the NCA was completely dissolved. The hot solution was cooled with an ice bath leading to the formation of many small crystals. (*Method b*) In the quest to obtain bigger crystals we added heptane to the hot clear ethyl acetate solution of the NCAs until precipitation was observed, followed by one drop of ethyl acetate whereupon the crystals again dissolved to obtain significantly larger crystals upon slow cooling down. For both methods the resulting crystals were filtered and washed with heptane. After drying in vacuum, the crystals were transferred to a glovebox for storage and polymerization. The procedure was performed at least three times to obtain highly pure crystals. In case of Aib-NCA the crystals obtained by both preparation methods (*a*, *b*) yielded the identical crystal structure as observed by XRD (Figure 1A), whereas for ACHC-NCA only crystals obtained by slow cooling from a heptane/ethyl acetate solution (*Method b*) yielded reasonably large single crystals with a highly ordered crystal structure (Figure 1C).

The similarly prepared Aib-NCA crystals have a needle like shape and can be prepared in different sizes depending on the crystallization method. *Method a* leads to an average length 1.36 mm ± 0.61 mm and width 0.21 mm ± 0.07 mm while *Method b* leads to bigger crystals with an average length 2.81 mm ± 1.47 mm and width 1.07 mm ± 0.36 mm. The crystals show a preference in the growing direction along the *a-axis* for all Aib-NCA crystals. Crystals obtained by *Method b* were highly ordered and the crystal lattice arrangement could easily be analyzed. The single crystal structure of the Aib-NCA (Figure 1A) shows a distance between the amine group and the carbonyl group of the next NCA of 4.16 Å in the same layer along the *c-axis*, a distance of 4.71 Å along the

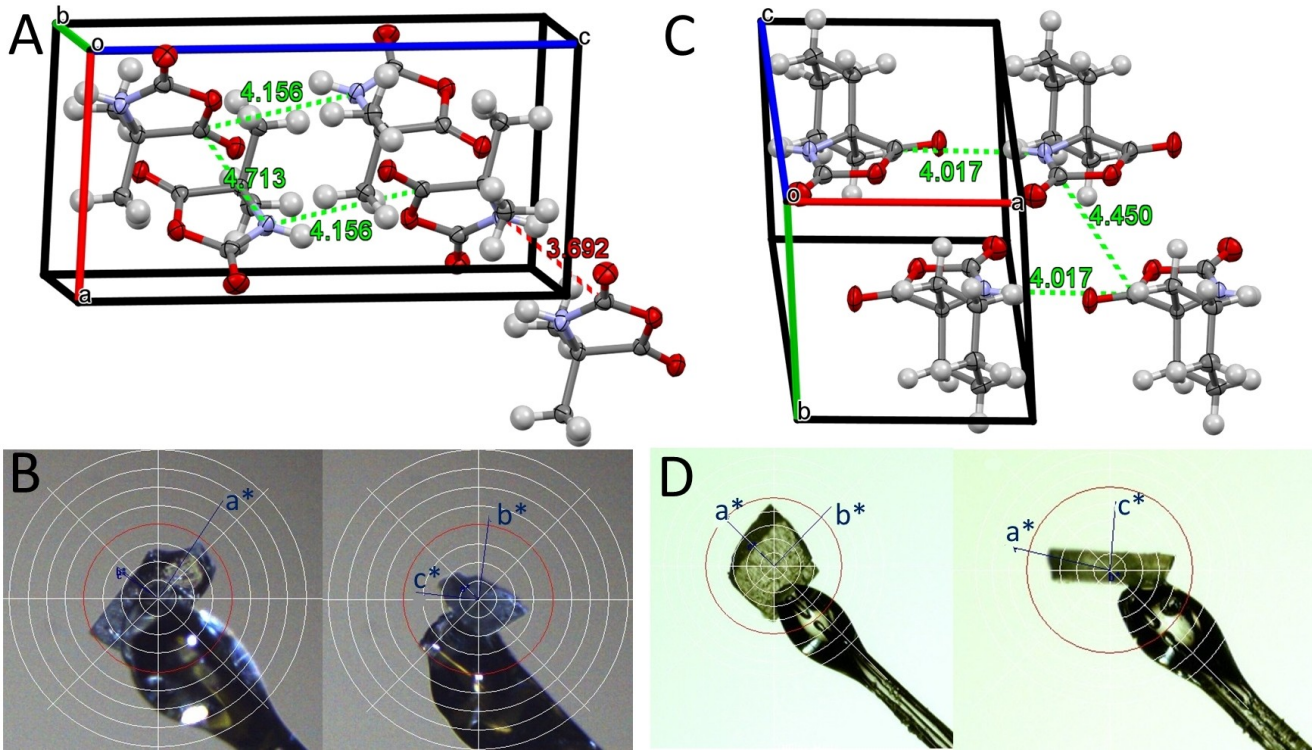

Figure 1. Single crystal structures of NCAs with oxygen atoms displayed in red and nitrogen atoms in light blue with distances measured and labelled in green between the amine group and the carbonyl group of a neighboring NCA in the crystal. The atoms in the crystal structure are shown as ellipsoids with anisotropic displacement parameters representing a 50% probability limit. A) The single crystal structure of Aib-NCA (Monoclinic space group P $2_1/c$) shows a dimerization in the crystal with the shortest distances being 3.69 Å between the dimerized NCAs indicated in red and 4.16 to 4.71 Å along the possible polymerization route indicated in green. B) Photographs of the measured Aib-NCA crystal with indication of the reciprocal lattice axis. C) The single crystal structure of ACHC-NCA (Monoclinic space group P $2_1/m$) displaying a layered structure with distances between 4.02 to 4.45 Å along a possible polymerization route through the crystal. D) Photographs of the measured ACHC-NCA crystal with the reciprocal lattice axis.

Table 1. Reaction conditions for NCAs in solution polymerization or topochemical single crystal polymerization by surface initiation. The used temperature and reaction time as well as obtained chain lengths determined by MALDI-ToF MS and the number average molecular weight (M_n) and polydispersity index (PDI) from the GPC are shown here for a small selection of reactions. The side reaction intensity was determined in the MALDI-ToF MS as percentage from the highest peak in the spectra. A full list of reactions is given in the Supporting Information Table S1.

Entry[a]	Polymer	Monomer	n_{aim}	Temperature [°C]	Time [days]	Yield [%]	Chain length (GPC M_n in g/mol; PDI)	Side reaction signal intensity[d] [%]
1	**Aib-1**	Aib-NCA Solution in DMF	150	80	1	48.8	11–32 (1444; 1.496)	6.2
2	**Aib-2**	Aib-NCA crystals[b]	30	rt	14	14.6	9–42 (1507; 1.169)	0.9
3	**Aib-3**	Aib-NCA crystals[b]	30	50	7	24.7	9–41 (1632; 1.245)	0.8
4	**Aib-4**	Aib-NCA crystals[b]	excess	rt	14	56.3	5–21 (1343; 1.099)	1.4
5	**Aib-5**	Aib-NCA small crystals[c]	30	rt	7	16.6	9–33 (1653; 1.167)	1.1
6	**ACHC-1**	ACHC-NCA Solution in DMF	150	80	1	15.4	8–30 (1244; 1.414)	7.5
7	**ACHC-2**	ACHC-NCA crystals	30	rt	7	7.3	5–50 (1601; 1.199)	1.2
8	**ACHC-3**	ACHC-NCA crystals	30	50	7	24.2	3–4 (1105; 1.442)	0.9

[a] The entry numbers of the Aib and ACHC polymers is continued in the full list of polymerizations in Table S1. [b] Aib-NCA crystals prepared with *Method b.* [c] Aib-NCA crystals prepared with *Method a.* [d] Determined by the Data-Analysis-program (Bruker) from MALDI-TOF data.

b-axis jumping between the upper and the lower layer, and 5.35–5.86 Å along the *a-axis*. Bonds along these axes indicated distances can lead to the formation of a polymer chain. The smallest distance between an amine and a carbonyl group in neighboring NCAs is those to the carbamic-carbonyl-group with only 3.69 Å, close enough to form hydrogen bonds, but preferring dimer formation instead of chain propagation (distance indicated in red in Figure 1 A). Dimerization via hydrogen bonding is said to potentially reduce the reactivity and prevent polymerization by hindering the movement of the NCA rings.[16] Additionally the attack angle of the nucleophilic amine onto the carbonyl group is 38.1° for the polymerization along the *c-axis* (distance 4.16 Å) and 25.5° for the polymerization along the *b-axis* (distance 4.71 Å). Both of these attack angles differ greatly from the Bürgi-Dunitz angle of 107° for an optimal nucleophilic attack.[22] Overall, the distances are in a suitable range for a topochemical polymerization with preferences along the c and b axis, but with uncertainty about their reactivity due to their topological arrangement and dimer formation.

In a similar mode the ACHC-NCA crystals were prepared and investigated by light-microscopy and XRD. The plate-shaped crystals are manly growing in the *a–b plane* (average edge length of 1.60 mm ± 0.64 mm) while the growth along the *c-axis* (average thickness 0.17 mm ± 0.04 mm) seems hindered (Figure 1 D). Single crystal investigation with XRD shows that the reactive 5 membered NCA rings are forming parallel layers along the a–b plane (Figure 1 C). The distance of 4.02 Å between the amine group and the carbonyl atom next to the α-carbon atom of the next NCA along the *a-axis* is in a suitable range for polymerization but the attack angle of amine is only 18.3°. This distance is sufficiently small to form hydrogen bonding bridges between the reactive centers of the NCA rings, leading to a possible pre-alignment for the future polymer bond along the *a-axis*. At the same time the distance to the next NCA ring layer along the b axis is 4.45 Å and the attack angle is 65.9°. With a difference of only 0.43 Å but a much broader angle for the attack there is a potential for polymerization to proceed in two different directions, leading to loss of order. The six membered rings are aligned in rows along the *a–b plane*, potentially acting as a separating layer and stopping polymerization along the c axis. Overall, the layered arrangement of the NCA rings and the hydrogen bonding between the correct reactive centers are making the ACHC-

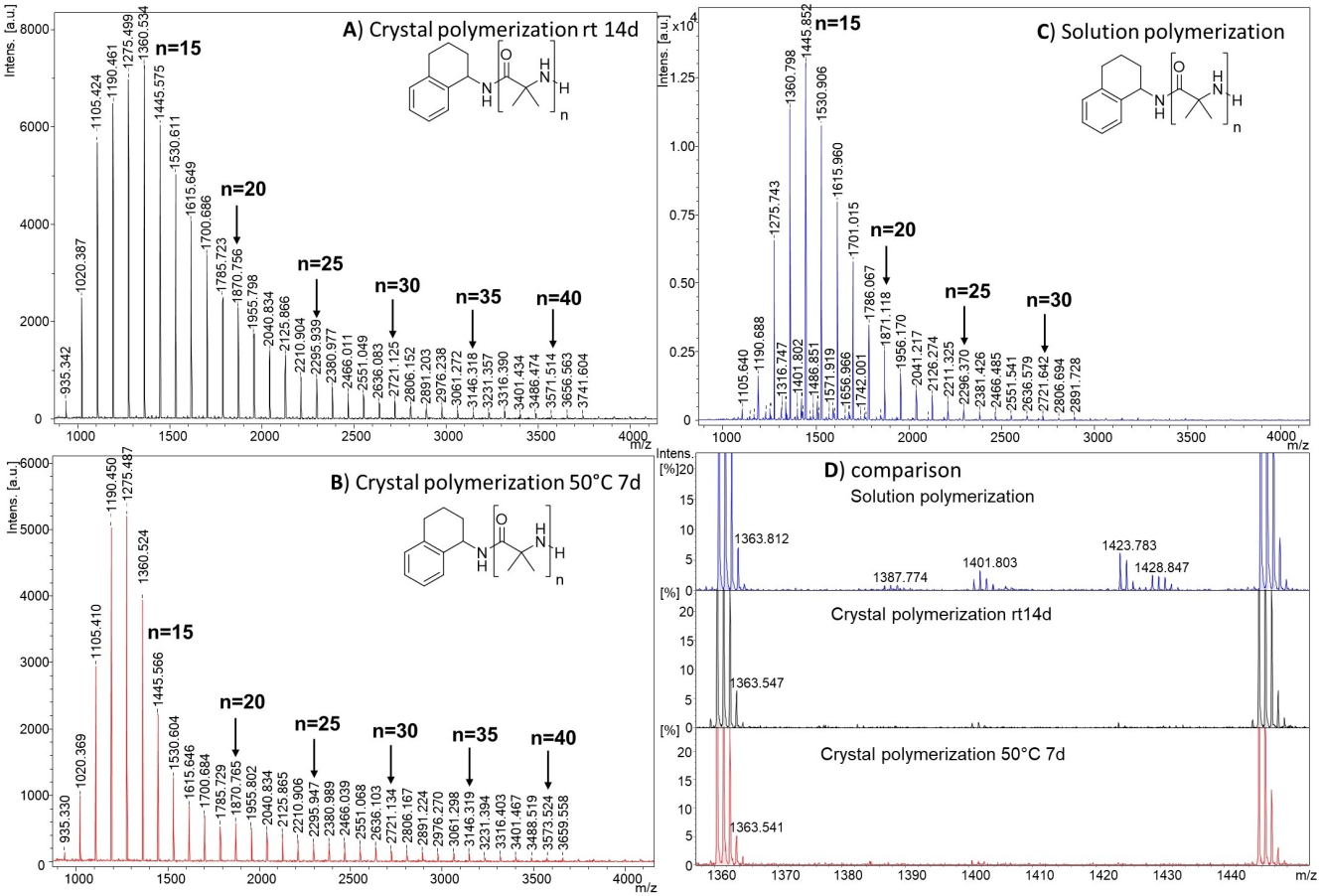

Figure 2. MALDI-ToF MS measurements of poly(Aib)s obtained by topochemical crystal polymerization A) at room temperature (entry 2 **Aib-2**-black) or B) at 50 °C (entry 3 **Aib-3**-red) and C) by solution polymerization (entry 1 **Aib-1**-blue). D) A zoomed in version is displayed to compare the results of the polymerization methods. The topochemical ROP results in polymers with higher chain length and without the side reactions which are clearly visible in the solution polymerization.

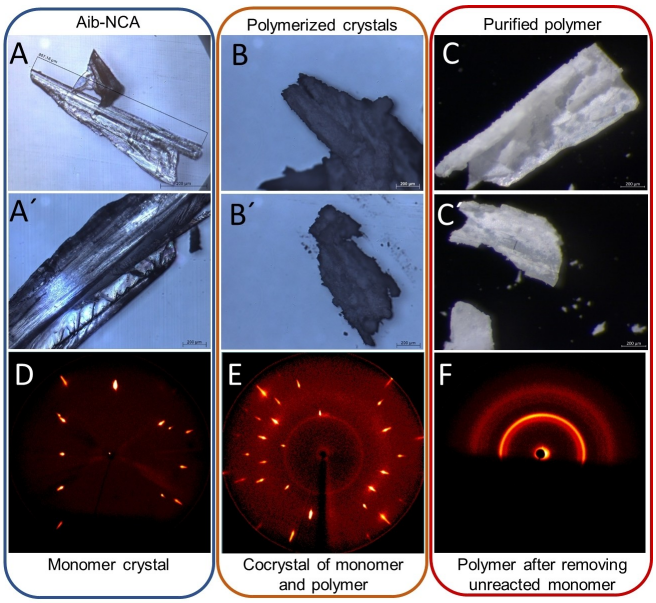

Figure 3. A) Microscopic pictures of single crystals of Aib-NCAs, B) the polymerized crystals and C) purified poly(Aib) crystals with D, E, F) their corresponding XRDs. Monomer crystals of Aib-NCA have a smooth surface and the XRD shows sharp and intense reflexes indicating a single crystalline structure. After the polymerization the crystals are rougher and show changed XRD patterns. The purified polymer has missing parts where the unreacted Aib-NCA was washed out and the corresponding XRD shows no long ordered structure anymore.

NCA a very promising candidate for a topochemical polymerization along the *a*- and *b*-*axis*.

Solid state (topochemical) ROP

To study the topochemical ROP, the NCA crystals were placed in a diluted initiator solution with heptane in which the NCA crystals are not soluble, assuming that the amines attack at the crystal surface, in turn initiating the topochemical ROP. Polymerizations were conducted in a glove box at room temperature (rt) or 50 °C with different initiator amounts and compared to the solution polymerization in DMF. Results of the polymerization of Aib-NCA and ACHC-NCA are summarized in Table 1 (see Table S1 for the full list). Some general trends depending on the reaction conditions are noticeable in that topochemical ROP. A polymerization with a small, calculated amount of initiator solution (target chain length $n_{aim} = 30$ repeating units) was forming higher chain lengths (entry 2 **Aib-2**), while the reaction with a huge excess of initiator (crystals dispersed in 1 mL initiator solution) gave a higher yield (entry 4 **Aib-4**). An increase in temperature to 50 °C leads to an increased yield compared to room temperature polymerization (entry 3 **Aib-3** and entry 8 **ACHC-3**). The higher chain lengths of up to n = 50, combined with a high purity for both NCAs makes it obvious that the topochemical ROP is advantageous compared to the purely solution-based approach (entry 1 **Aib-1** and entry 5 **ACHC-1**).

To prove the progression of the ROP through the single crystal, forming poly(Aib) by an amine-initiated ROP, MALDI-ToF MS was used to check for the end group control and chain length (see Figure 2). The largest signals in all spectra could be assigned to poly(Aib) bearing the initiator at the C-terminus and a hydrogen at the N-terminus ionized with a sodium ion $[C_{10}H_{12}N(C_4H_7NO)_nH + Na]^+$. In order to compare the outcome of the topochemical ROP to those of a conventional solution ROP, we conducted the same ROP also in solution under known conditions, as reported by us recently.[21a,23] MALDI-ToF MS of the solution polymerization (Figure 2C, D) shows multiple side reactions occurring during the polymerization with an only limited molecular weight (n = 32) due to the poor solubility of the final polymer. In contrast there are no side reactions in the topochemical ROP as there are no signals besides the main series in the MALDI-ToF MS of the polymer, proving a perfect end group control and the absence of termination/chain transfer chemistries (Figure 2A and B). We are thus concluding that the polymerization proceeds in a living manner, as no chains devoid of the initiator could be found for the topochemical ROP. As already mentioned, the topochemical ROP also solved another drawback, well known from solution polymerization, where chain length is limited due to precipitation of the formed polymer, when e.g., conducted in DMF-solution. In contrast the chain length of topochemical polymerized poly(Aib)s detected in MALDI-ToF MS reaches up to over 45 repeating units, which is significantly longer compared to normal solution polymerization.[21a] We also investigated the ROP conducted in crystals of different size: for Aib-NCA two crystal sizes were investigated, both leading to polymers by topochemical ROP, both yielding a higher maximum chain length and purity for bigger crystals obtained by *Method b* (see Table 1 entry 2 **Aib-2**) compared to a polymerization of small crystals obtained by *Method a* (see Table 1 entry 5 **Aib-5**). The high purity polymers resulting from the bigger-sized Aib-NCA crystals were subsequently investigated with light-microscopy and XRD.

For Aib-NCA light microscopy shows a needle like shape with smooth shiny surfaces (Figure 3A); in XRD (Figure 3D) very sharp and intense reflexes proofing a perfectly order single crystal. After polymerization the surfaces of the crystals displayed a morphological change, indicating that the polymerization distorts the crystal surfaces, which are now appearing rough and frosted (Figure 3B). As observed by XRD more reflexes appear and an isotropic ring is formed with progressing ROP (Figure 3E). Most of the sharp reflexes can be assigned to unreacted Aib-NCA and the additional reflexes indicate a breaking of the single crystal with further distortion of the lattice by the generated polymer. The polymer itself generates an isotropic ring scattering pattern, similar to the later observed XRD of the purified polymer (see Figure 3F, obtained from measurement on solid support, i.e., only upper hemisphere is visible). After purification of the polymerized crystal with ACN the solid polymer

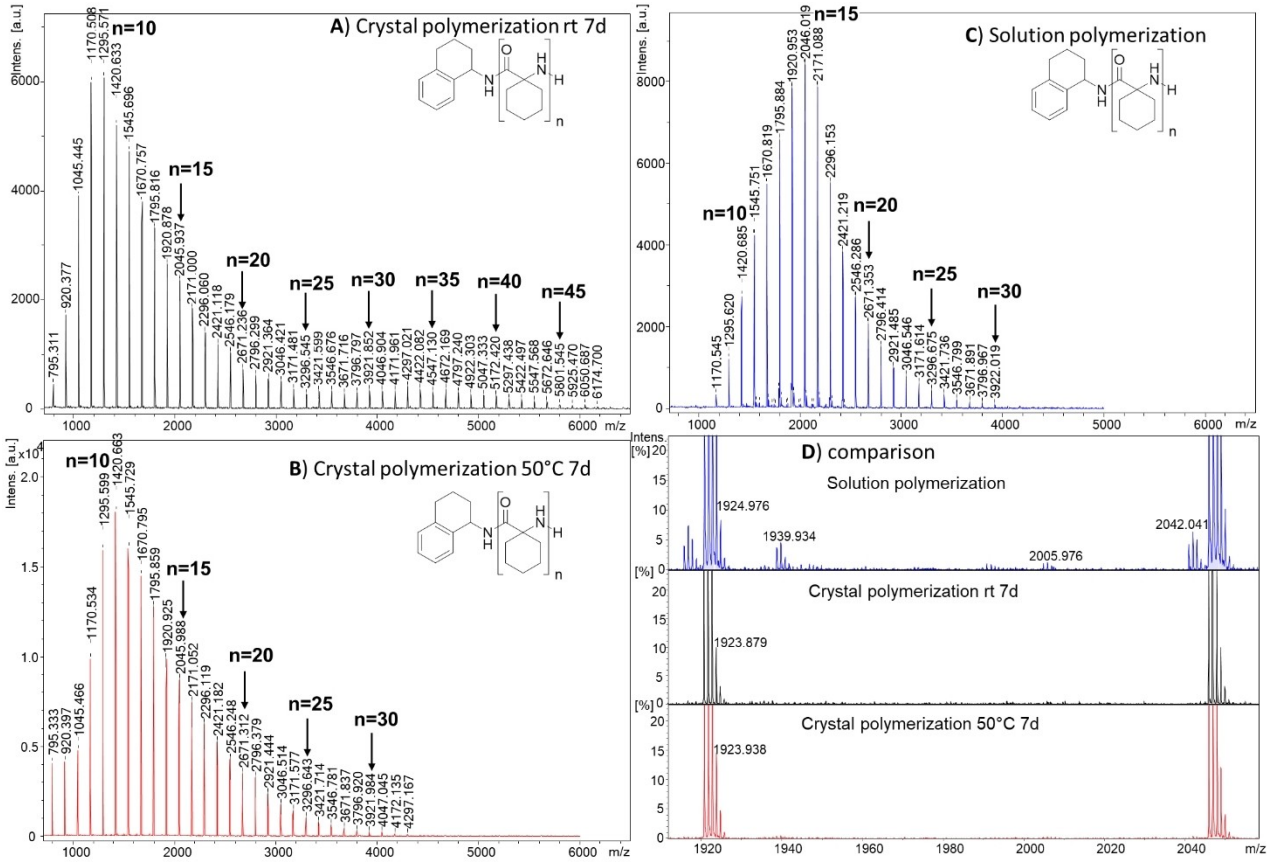

Figure 4. MALDI-ToF MS measurements of poly(ACHC)s obtained by topochemical crystal polymerization A) at room temperature (entry 7 **ACHC-2**-black) or B) at 50 °C (entry 8 **ACHC-3**-red) and C) by solution polymerization (entry 6 **ACHC-1**-blue). D) A zoomed in version is displayed to compare the results of the polymerization methods. The topochemical ROP results in polymers with higher chain length and without the side reactions which are clearly visible in the solution polymerization.

was directly obtained, as the unreacted monomer dissolved leaving the polymer behind (Figure 3C).

The Aib-NCA seems to be highly reactive in the single crystal state even though it forms a dimer with hydrogen bonds which is said to be lowering the reactivity. The pre-alignment of the NCAs and the high purity of the single crystal are enhancing the ROP of Aib-NCA, breaking the limitations of the solution ROP.

In a similar mode the ACHC-polymers formed by topochemical ROP were analyzed with MALDI-ToF MS (see Figure 4A, B) to confirm their purity and chain length. The main signals in all MALDI-ToF MS could be assigned to a series of poly(ACHC), bearing the initiator at the C-terminus and hydrogen at the N-terminus plus a sodium ion $[C_{10}H_{12}N\text{-}(C_{10}H_7NO)_nH + Na]^+$. MALDI-ToF MS of the polymer obtained by solution polymerization (Figure 4C, D) shows side reaction peaks, not present anymore in the topochemical polymerized poly(ACHC)s. The detected chain lengths of topochemical polymerized poly(ACHC) ranges up to $n = 50$ repeating units without significant side reactions visible as seen in the MALDI-ToF MS (Figure 4D). The purity of the poly(ACHC) is as high as those of poly(Aib) obtained by topochemical single-crystal polymerization, underrscoring the high potential of topochemical ROP of NCAs.

Similar to the topochemical ROP of the Aib-NCAs, single crystals of ACHC-NCA were investigated with light-microscopy and XRD and were polymerized via amine-based initiation. The plate-like monomer crystals display a flat and smooth surface, which become rougher during polymerization (Figure 5A, B and C). A transition in XRD was also observed moving from a highly ordered single crystal with sharp and intense reflexes to a complete loss of the long-range ordered structure and a ring-like signal (Figure 5D, E and F). The polymerization is likely proceeding through the crystal along the a and b axis leading to a polymer with partially crystalline structure, but without preferred orientation.

We further probed the transfer of chirality in this topochemical process, using a chiral amine as initiator. Chiral head groups are known to transform the otherwise achiral poly(Aib) and poly(ACHC) chains into regular helical folds, with preferential helicity by head-group interactions.[21a,24] As we have used the chiral initiator *R*-/*S*-1,2,3,4-tetrahydro-1-naphthylamine as a chiral inductor, we probed the formation of either left- or right-handed helices. CD spectroscopy (Figure 6) shows excellent mirror-images between the corresponding *R*- and *S*-amine initiated polymers in either HFIP or a water/HFIP (95/5) mixture. The CD

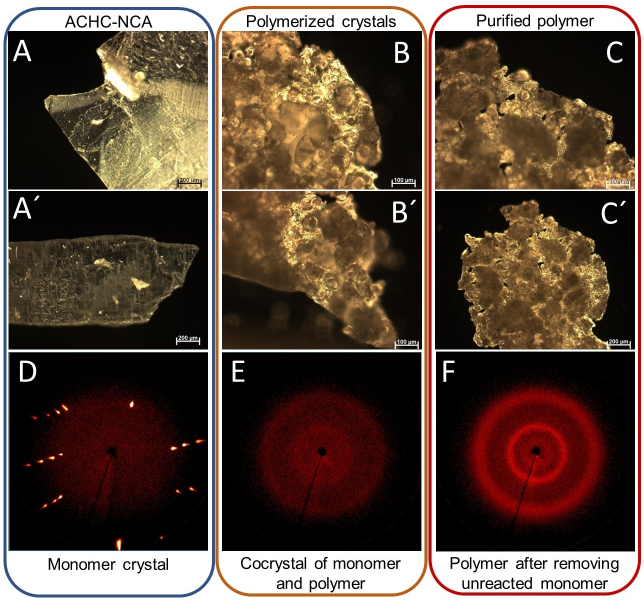

Figure 5. Microscopic pictures of single crystals of ACHC-NCA, polymerized crystals and purified poly(ACHC) crystals with their corresponding XRDs. A) Monomer crystals of ACHC-NCA have sharp edges with a flat, smooth surface and D) the XRD shows sharp and intense reflexes indicating a single crystalline structure. B) After polymerization the crystals are rougher and show E) a changed XRD pattern with the loss of the long order. C) The purified polymer shows small holes where the unreacted ACHC-NCA was washed out with F) the corresponding XRD, for poly(ACHC) with rotating crystal measurement.

spectra are similar to previously reported CD spectroscopy investigations[21a] and thereby prove that chirality transfer is independent of the polymerization technique used, also indicating that the topochemical ROP is proceeding with an excellent degree of head-group incorporation.

Conclusions

In this article we report for the first time the preparation and analysis of Aib-NCA and ACHC-NCA single crystals and their topochemical ring-opening polymerization. The polymerization was conducted directly in the single crystal by initiating directly at the crystal surface, followed by monomer-removal by washing with acetonitrile to generate the solid polymer. MALDI-ToF MS revealed significantly increased chain length and the absence of side reactions during the polymerization when compared to solution polymerization. We also observed livingness of the polymerization, with a precise attachment of the initiator to every polymer chain, as proven by MALDI-ToF MS. The distances between the reactive centers of two NCAs are between 4 and 5 Å and thus well in the range of previously reported topochemical single crystal polymerizations, with layered structures for the ACHC-NCA, being advantageous for polymerization as reported previously. For Aib-NCA, even though this NCA would be poorly polymerizable due to dimer formation, we were able to achieve pure poly(Aib) with excellent chain length. The quite good polymerizability of Aib-NCA stays in contrast to the reportedly poor polymerizability of the glycine-NCA, which also exhibits a dimerization in the crystal lattice. When analyzing the XRD data and the morphological changes of the crystals during the polymerization it is safe to assume that the evolving carbon dioxide as well as the newly forming polymer chain are leading to local distortions in the crystal lattice, hindering the propagation of the polymerization while following the crystals lattice. Therefore, this ROP of NCAs in the crystal state can be regarded as a special type of a topochemical polymerization with an unusual initiation by a surface attack of an amine. However, the improved purity and higher chain lengths, compared to conventional solution polymerization, makes this method a promising candidate to produce highly pure poly(amino acids), additionally obtaining excellent chiral induction on these achiral polymers with a chiral amines.

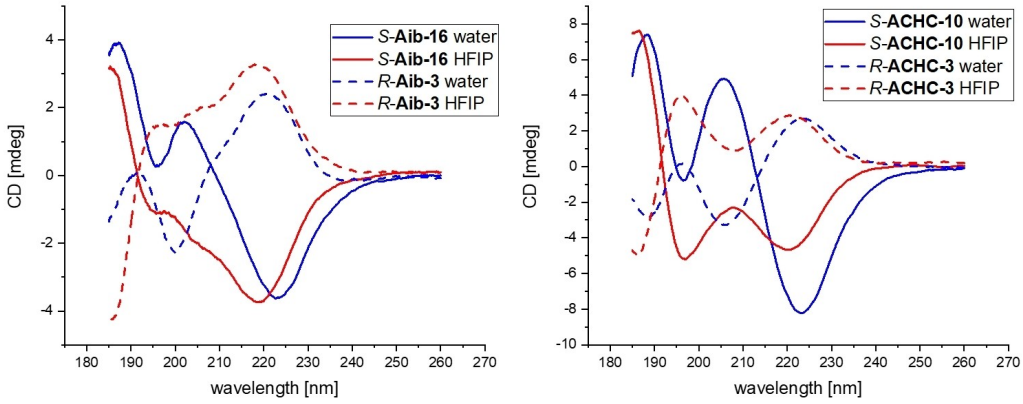

Figure 6. CD investigations in HFIP (red) or water/HFIP 95/5 (blue) of poly(Aib) and poly(ACHC) obtained by topochemical ROP with *R*- or *S*-1,2,3,4-tetrahydro-1-naphthylamine as an initiator.

Experimental Section

Aib-NCA and ACHC-NCA were prepared with triphosgene in ethyl acetate following the literature procedure.[21b] The solution ROP of the NCAs was conducted in DMF at 80 °C like previously reported.[21a] To conduct the topochemical ring-opening polymerization, the NCA single crystals were placed in a diluted amine solution and were polymerized over several days at room temperature or 50 °C. Further details for all reactions as well as the materials and method description are given in the Supporting Information.

Deposition Numbers 2266201 (for Aib-NCA) and 2266299 (for ACHC-NCA) contain the supplementary crystallographic data for this paper. These data are provided free of charge by the joint Cambridge Crystallographic Data Centre and Fachinformationszentrum Karlsruhe Access Structures service.

Acknowledgements

DFG Project B 1337/16-7. Open Access funding enabled and organized by Projekt DEAL.

Conflict of Interests

The authors declare no conflict of interest.

Data Availability Statement

The data that support the findings of this study are available in the supplementary material of this article.

Keywords: achiral amino acid · MALDI-ToF MS · ring-opening polymerization · single crystals · topochemical polymerization

[1] a) K. Hema, A. Ravi, C. Raju, J. R. Pathan, R. Rai, K. M. Sureshan, *Chem. Soc. Rev.* **2021**, *50*, 4062–4099; b) S. Naskar, R. Moi, I. Das, K. Biradha, *Angew. Chem. Int. Ed.* **2022**, *61*, e202204141; c) S. Khan, A. Frontera, R. Matsuda, S. Kitagawa, M. H. Mir, *Inorg. Chem.* **2022**, *61*, 3029–3032; d) M. Hasegawa, *Pure Appl. Chem.* **1986**, *58*, 1179–1188; e) M. Hasegawa, *Chem. Rev.* **1983**, *83*, 507–518; f) H. Nakanishi, W. Jones, J. M. Thomas, M. Hasegawa, W. L. Rees, *Proc. R. Soc. Lond. A* **1980**, *369*, 307–325.
[2] a) R. Rai, B. P. Krishnan, K. M. Sureshan, *Proc. Natl. Acad. Sci. USA* **2018**, *115*, 2896–2901; b) R. Khazeber, K. M. Sureshan, *Angew. Chem. Int. Ed.* **2021**, *60*, 24875–24881; c) K. Hema, C. Raju, S. Bhandary, K. M. Sureshan, *Angew. Chem. Int. Ed.* **2022**, *61*, e202210733; d) K. Hema, K. M. Sureshan, *Angew. Chem. Int. Ed.* **2020**, *59*, 8854–8859.
[3] F. Li, J. Xu, Y. Wang, H. Zheng, K. Li, *Molecules* **2021**, *26*, 7581.
[4] a) Z. Wei, X. Wang, B. Seo, X. Luo, Q. Hu, J. Jones, M. Zeller, K. Wang, B. M. Savoie, K. Zhao, L. Dou, *Angew. Chem. Int. Ed.* **2022**, *61*, e202213840; b) C. L. Anderson, H. Li, C. G. Jones, S. J. Teat, N. S. Settineri, E. A. Dailing, J. Liang, H. Mao, C. Yang, L. M. Klivansky, X. Li, J. A. Reimer, H. M. Nelson, Y. Liu, *Nat. Commun.* **2021**, *12*, 6818; c) J. W. Lauher, F. W. Fowler, N. S. Goroff, *Acc. Chem. Res.* **2008**, *41*, 1215–1229; d) G. Wegner, *Macromol. Symp.* **1996**, *101*, 257–264; e) B. Tieke, G. Lieser, G. Wegner, *J. Polym. Sci. Polym. Chem. Ed.* **1979**, *17*, 1631–1644; f) W. Hersel, H. Sixl, G. Wegner, *Chem. Phys. Lett.* **1980**, *73*, 288–293; g) M. Rosenthal, L. Li, J. J. Hernandez, X. Zhu, D. A. Ivanov, M. Möller, *Chem. Eur. J.* **2013**, *19*, 4300–4307.
[5] K. Morimoto, D. Kitagawa, H. Sotome, S. Ito, H. Miyasaka, S. Kobatake, *Angew. Chem. Int. Ed.* **2022**, *61*, e202212290.
[6] X. Yang, X. Wang, Y. Wang, K. Li, H. Y. Zheng, *Crystals* **2019**, *9*, 490.
[7] a) S. Agbolaghi, S. Abbaspoor, F. Abbasi, *Prog. Polym. Sci.* **2018**, *81*, 22–79; b) F. Hu, X. W. Bi, X. S. Chen, Q. Y. Pan, Y. J. Zhao, *Chem. Lett.* **2021**, *50*, 1015–1029; c) L. Peng, Q. Guo, C. Song, S. Ghosh, H. Xu, L. Wang, D. Hu, L. Shi, L. Zhao, Q. Li, T. Sakurai, H. Yan, S. Seki, Y. Liu, D. Wei, *Nat. Commun.* **2021**, *12*, 5077; d) Q. H. Guo, M. Jia, Z. Liu, Y. Qiu, H. Chen, D. Shen, X. Zhang, Q. Tu, M. R. Ryder, H. Chen, P. Li, Y. Xu, P. Li, Z. Chen, G. S. Shekhawat, V. P. Dravid, R. Q. Snurr, D. Philp, A. C. Sue, O. K. Farha, M. Rolandi, J. F. Stoddart, *J. Am. Chem. Soc.* **2020**, *142*, 6180–6187.
[8] a) K. Hema, A. Ravi, C. Raju, K. M. Sureshan, *Chem. Sci.* **2021**, *12*, 5361–5380; b) E. Jahnke, J. Weiss, S. Neuhaus, T. N. Hoheisel, H. Frauenrath, *Chem. Eur. J.* **2009**, *15*, 388–404.
[9] K. Biradha, R. Santra, *Chem. Soc. Rev.* **2013**, *42*, 950–967.
[10] S. Fang, S. Y.-L. Leung, Y. Li, V. W.-W. Yam, *Chem. Eur. J.* **2018**, *24*, 15596–15602.
[11] A. Matsumoto, *Polym. J.* **2003**, *35*, 93–121.
[12] Y. Oaki, K. Sato, *J. Mater. Chem. A* **2018**, *6*, 23197–23219.
[13] a) J. G. Nery, G. Bolbach, I. Weissbuch, M. Lahav, *Angew. Chem. Int. Ed.* **2003**, *42*, 2157–2161; b) J. G. Nery, R. Eliash, G. Bolbach, I. Weissbuch, M. Lahav, *Chirality* **2007**, *19*, 612–624; c) R. Eliash, J. G. Nery, I. Rubinstein, G. Clodic, G. Bolbach, I. Weissbuch, M. Lahav, *Chem. Eur. J.* **2007**, *13*, 10140–10151.
[14] H. R. Kricheldorf, *Angew. Chem. Int. Ed.* **2006**, *45*, 5752–5784.
[15] H. Kanazawa, Y. Ohashi, Y. Sasada, T. Kawai, *J. Polym. Sci. Polym. Phys. Ed.* **1982**, *20*, 1847–1862.
[16] H. Kanazawa, T. Kawai, *J. Polym. Sci. Polym. Chem. Ed.* **1980**, *18*, 629–642.
[17] H. Kanazawa, *in Advances in Organic Crystal Chemistry*, Springer Japan, **2015**, p. 503–515.
[18] J. G. Nery, G. Bolbach, I. Weissbuch, M. Lahav, *Chem. Eur. J.* **2005**, *11*, 3039–3048.
[19] a) H. Zepik, E. Shavit, M. Tang, T. R. Jensen, K. Kjaer, G. Bolbach, L. Leiserowitz, I. Weissbuch, M. Lahav, *Science* **2002**, *295*, 1266–1269; b) I. Weissbuch, G. Bolbach, L. Leiserowitz, M. Lahav, *Origins Life Evol. Biospheres* **2004**, *34*, 79–92.
[20] H. Kanazawa, *in Encyclopedia of Polymeric Nanomaterials* (Eds.: S. Kobayashi, K. Müllen), Springer Berlin Heidelberg, Berlin, Heidelberg, **2015**, p. 1972–1982.
[21] a) M. Rohmer, O. Ucak, R. Fredrick, W. H. Binder, *Polym. Chem.* **2021**, *12*, 6252–6262; b) J. Freudenberg, W. H. Binder, *ACS Macro Lett.* **2020**, *9*, 686–692.
[22] H. B. Burgi, J. D. Dunitz, E. Shefter, *J. Am. Chem. Soc.* **1973**, *95*, 5065–5067.
[23] M. Rohmer, J. Freudenberg, W. H. Binder, *Macromol. Biosci.* **2023**, *23*, e2200344.
[24] a) F. G. A. Lister, B. A. F. Le Bailly, S. J. Webb, J. Clayden, *Nat. Chem.* **2017**, *9*, 420–425; b) L. Byrne, J. Sola, T. Boddaert, T. Marcelli, R. W. Adams, G. A. Morris, J. Clayden, *Angew. Chem. Int. Ed.* **2014**, *53*, 151–155.

Manuscript received: August 18, 2023
Accepted manuscript online: September 12, 2023
Version of record online: October 24, 2023